



Tryptamine and CMC-Na modified gel for Fe³⁺ adsorption in water

Jiaming Hu^a, Shuai Zhang^a, Chen Feng^a, Shanggen Li^{a,b}, Longfei Zhang^{a,c},
Jiajun Ma^c, Qiang Yin^{a,*}

^aResearch Center of Laser Fusion, China Academy of Engineering Physics, Mianyang 621900, Sichuan, China, Tel. +86-2488462; Fax: 0816-2493148; email: qyin839@163.com (Q. Yin), Tel. +86-08162482760; email: 1306853353@qq.com (J. Hu), Tel. +86-08162488462; email: zhangshuai_scu@126.com (S. Zhang), Tel. +86-08162482760; emails: 1105749162@qq.com (C. Feng), lsglsg@mail.usc.edu.cn (S. Li), flz@mail.usc.edu.cn (L. Zhang)

^bDepartment of Engineering and Applied Physics, University of Science and Technology of China, Hefei 230026, Anhui, China

^cState Key Laboratory of Environment-friendly Energy Materials & School of Material Science and Engineering, Southwest University of Science and Technology, Mianyang 621010, Sichuan, China, Tel. +86-08162488462; email: majiajun@swust.edu.cn

Received 24 March 2021; Accepted 21 June 2021

ABSTRACT

In this work, an efficient Fe³⁺ adsorbent was synthesized by using the tryptamine and sodium carboxymethyl cellulose (CMC-Na) modified polyacrylamide gel. The functional monomers synthesized by the reaction of tryptamine and methacrylic acid chloride were doped into the composition, and CMC-Na participated in the formation of the gel network. By changing different conditions, the optimal use conditions of the gel were explored. The Langmuir and Freundlich isotherm models were used to discuss the adsorption behavior. According to the fitting results, the Freundlich model was more suitable for explaining the adsorption of Fe³⁺ by gels. The feasibility of its adsorption process was confirmed by the study of its kinetics and thermodynamics. As an adsorbent, tryptamine CMC-Na modified polyacrylamide gel has excellent ability to remove Fe³⁺ from aqueous solutions. The maximum adsorption capacity of tryptamine and CMC-Na modified polyacrylamide gel for Fe³⁺ reached 127.5 mg g⁻¹.

Keywords: Adsorption; CMC-Na; Fe³⁺; Gel; Modified; Tryptamine

1. Introduction

Metallurgy and mining industries will produce a lot of heavy metal ion pollution, such as Fe³⁺, Cu²⁺, Pb²⁺, and Cd²⁺, which will have serious impacts on the ecological environment [1,2]. These metal ions cannot be biodegraded and will damage the ecosystem, and their high concentration accumulation in organisms can cause toxicity to plants, animals, and humans. Among them, iron, as an essential metal element, has received more and more attention in biological and environmental systems.

In many industrial processes, iron or impurities must be removed from the solution, and removing iron is

also one of the processes for producing drinking water. The main problems of iron pollution involve discoloration of water, deterioration of water taste, and clogging of pipes. Pollutants in the metallurgical industry and steel-making industry are the main cause of iron pollution in surface water. Iron promotes the growth of “iron bacteria” and deposits a thick coating on the pipe. In freshwater, the concentration of iron is usually 0–50 mg L⁻¹ [3]. When the iron content exceeds 0.3 mg L⁻¹, iron can stain clothes and contaminate equipment. Iron dissolved in water will reduce the quality of water, for example, the color of the water changes to red and produces an unpleasant smell of rust [4]. Too much or too little iron intake will have certain effects

* Corresponding author.

on the organism. Too much iron can accumulate in certain organs (such as liver, bone marrow, and skin), leading to dysfunction [5]. Corroded iron pipes or residual iron-based coagulants will dissolve iron and seep into the ground, resulting in increased iron content in groundwater.

At present, methods for treating iron in water include electrocoagulation (EC) [6], oxidation/filtration [7], ion exchange [8], and the use of activated carbon and other filter materials [9] to adsorb Fe^{3+} in water. In terms of electrocoagulation, Subramanian uses zinc as the cathode and anode to remove iron in water under AC and DC conditions, with a removal efficiency of 99% [10]. In addition, Subramanian also uses aluminum alloy as anode and stainless steel as cathode to remove iron from drinking water, achieving a maximum removal efficiency of 98.8% [11]. Most iron treatment systems currently use oxidation/filtration processes. The oxidant chemically oxidizes the iron (forming a particle) and kills iron bacteria. The filter then removes the iron particles, in this process, the water source must be monitored to determine the appropriate amount of oxidant, and the treated water should be monitored to determine whether the oxidation process is successful. Ion exchange involves the use of synthetic resins in which pre-saturated ions on the solid phase are exchanged for unwanted ions in the water. One of the main difficulties in using this method to control iron and manganese is that if any oxidation occurs during this process, the resulting sediment will cover and contaminate the medium. The adsorption method is considered to be a simple, effective, economical, convenient, and environmentally friendly method for removing Fe^{3+} . One of the most effective ways to remove these pollutants is to use activated carbon. Activated carbon and other carbon-containing materials are excellent adsorbents with cost-effectiveness, high porosity, and large specific surface area, and have been widely used in wastewater treatment [5,12–14]. However, the recovery of activated carbon is relatively difficult, and its high regeneration cost limits its application, which makes its practical application slightly difficult. Therefore, it is necessary to develop a new type of adsorbent to adsorb Fe^{3+} in the recovered water.

Nitrogen-containing heterocyclic compounds are widely found in natural products [15] and biomolecules [16]. Among these compounds, indole is a highly active, electricity-rich heterocyclic compound with a special structure, and it exists in various biomolecules and

pharmaceutical molecules, pesticides, dyes, and essential oils [17,18]. Indole also has a typical π -electron-rich aromatic system [19,20], which can be used as active sites for supplying electron-deficient groups and cations. For example, indole-based porous organic polymers pass through local dipoles- π interaction shows a strong adsorption capacity for polarizable carbon dioxide (CO_2) [21,22]. Taking advantage of the electron-rich properties of indole, Zhang et al. [23] prepared a renewable 4-HIF/NaOH aerogel, which can effectively remove methylene blue through electrostatic interaction induced by cation- π interaction. Wang et al. [24] also constructed indole-based aerogel 4-AING and used it for simultaneous visual detection and removal of TNT in aqueous systems. What's more, some absorbent materials prepared by biological macromolecules containing functional groups such as $-\text{COOH}$ and $-\text{OH}$ also have excellent adsorption properties for transition metal ions [25,26].

Based on this, we introduced the two substances containing the above functional groups in our work, using acrylamide with good water-absorption capacity as the basic skeleton of the gel, and reacting tryptamine with indole group and methacrylic acid chloride is doped into the main chain. Sodium carboxymethyl cellulose (CMC-Na) is used to enhance the network structure of the gel, increase the water-absorption of the gel, and work with the indole group to adsorb Fe^{3+} . The design idea is shown in Fig. 1. The maximum adsorption capacity, pH value, adsorption time, initial concentration of Fe^{3+} and adsorption temperature, as well as the influence of competitive adsorption and other factors were carried out through batch experiments. In addition, we conduct systematic researches and discussion to understand the kinetics, isotherms, and thermodynamics of the prepared gel adsorption process. The improved gel has active groups such as indole and carboxyl group, which can be used as an adsorbent to adsorb Fe^{3+} , and the maximum adsorption capacity of tryptamine and CMC-Na modified polyacrylamide gel for Fe^{3+} reached 127.5 mg g^{-1} .

2. Methods and materials

2.1. Material

Tryptamine (98%), N,N'-methylenebisacrylamide (99%), ammonium persulfate (99.99%), acrylamide (99%), sodium carboxymethyl cellulose (viscosity: 800–1,200 mpa·s),

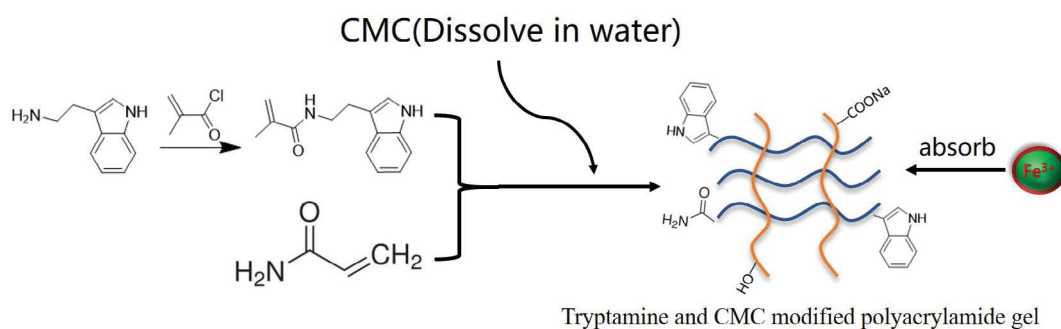


Fig. 1. Preparation process of tryptamine and CMC-Na modified polyacrylamide hydrogel.

methacryloyl chloride (95%), $\text{NiCl}_2 \cdot 6\text{H}_2\text{O}$ (AR), and $\text{CoCl}_2 \cdot 6\text{H}_2\text{O}$ (AR) were purchased from Aladdin Biochemical Technology Co., Ltd., (Shanghai, China); Triethylamine (99.5%) was purchased from Macklin Biochemical Technology Co., Ltd., (Shanghai, China); and FeCl_3 (97%) was purchased from Sigma-Aldrich Trading Co., Ltd., (Shanghai, China).

2.2. Synthesis of *N*-(2-(1*H*-indol-3-yl)ethyl)methacrylamide

Under argon atmosphere, tryptamine (5.0 g) and triethylamine (12 mL) were dissolved in dichloromethane, stirred at 0°C for 20 min, and methacrylic (3.9 g) acid chloride was added dropwise to the above solution, as soon as it returned to room temperature. After stirring for 12 h, the crude product was obtained. The crude product was washed three times with potassium carbonate solution and saturated brine, dried over anhydrous sodium sulfate. Purified by column chromatography (ethyl acetate: petroleum ether = 1:3) to obtain a yellow sticky liquid.

2.3. Preparation of gel

N-(2-(1*H*-indol-3-yl)ethyl)methacrylamide (0.1 g), acrylamide (0.83 g), and methylene-bis-acrylamide (0.03 g) were dissolved in DMSO (4 mL). After the dissolution was complete, add 3% CMC-Na aqueous solution (1 mL) dropwise. After mixed uniformly, reacted for 1 h at 80°C. After aging for 6 h at 80°C, replaced with deionized water for 7 d. The final product was obtained after freeze-drying.

2.4. Characterization

KBr was used to test the chemical structure of the gel on the Nicolet IS5 Fourier transform infrared spectroscopy (FT-IR). The Zeiss sigma 500 scanning electron microscope (SEM) was used to observe the microstructure of the gel. The chemical structure of the synthesized substance was analyzed on the Bruker Avance III HD 400 MHz proton nuclear magnetic resonance spectrum (NMR). The Thermo Scientific Escalab 250Xi (XPS) was used to characterize the changes of functional groups before and after the adsorption of hydrogels. An Agilent 720 inductively coupled plasma spectroscopy/mass spectrometry (ICP-AES/MS) was used to test the concentration of Fe^{3+} in the solution after adsorption.

2.5. Adsorption experiment

A batch of adsorption experiment was carried out systematically to evaluate the adsorption capacity of the gel to Fe^{3+} , including different initial pH, temperature, adsorption time, etc.

- In the pH study, adjust the pH of the Fe^{3+} solution to the required range with 1 M HCl and 1 M NaOH solution, and then add 10 mg of gel to the 200 mg L^{-1} Fe^{3+} solution sample bottle (10 mL), and then fully Mix and react at 30°C for 24 h.
- In the experiment of initial concentration, the concentration of Fe^{3+} solution for adsorption test was 50–300 mg L^{-1} , and gel (10 mg) is added to sample bottles (10 mL)

containing Fe^{3+} solutions of different concentrations. Then mix well and react at 30°C for 24 h.

- In the study of the contact time, after adjusting the pH value of the Fe^{3+} solution to the optimum pH with 1 M HCl and 1 M NaOH solution, the adsorption test was carried out. The concentration of the Fe^{3+} solution was 200 mg L^{-1} . After adding gel (10 mg), samples are taken at intervals and tested for a certain period time until the reaction reaches 10 h.
- In the adsorption kinetics and thermodynamic experiments, after adjusting the pH value of the Fe^{3+} solution to the optimum pH with 1 M HCl and 1 M NaOH solution, perform the adsorption test. The concentration of the Fe^{3+} solution was 50–300 mg L^{-1} , temperature from 298 to 313 K, reacted for 8 h.
- When performing competitive adsorption, mixed solutions with the same concentration of Co^{2+} , Cu^{2+} , Fe^{3+} , and Ni^{2+} , and reacted at 30°C for 8 h before testing.
- Conduct comparative adsorption experiments. The gel components contain CMC-Na, *N*-(2-(1*H*-indol-3-yl)ethyl) methacrylamide, and different mass ratio *N*-(2-(1*H*-indol-3-yl)ethyl)methacrylamide and CMC-Na gel was added to the 200 mg L^{-1} Fe^{3+} solution sample bottle (10 mL), and reacted for 8 h. The concentration of Fe^{3+} before and after adsorption was measured by atomic absorption spectrometry.

The calculation formula of adsorption capacity (q_e , mg g^{-1}) is as follows:

$$q_e = \left(\frac{C_0 - C_e}{m} \right) V \quad (1)$$

where C_0 and C_e are the initial and final concentrations of Fe^{3+} (mg L^{-1}), respectively. V is the volume (L) of the Fe^{3+} solution, and m is the weight (g) of the adsorbent. And linear regression analysis was used to verify the adsorption results.

3. Results and discussion

3.1. Characterization of *N*-(2-(1*H*-indol-3-yl)ethyl)methacrylamide

In order to obtain the ability to dope tryptamine in the gel backbone, tryptamine was reacted with methacrylic acid chloride. After obtaining the results, perform nuclear magnetic was analyzed. The ^1H -NMR spectrum (400 MHz, CDCl_3 , δ -ppm) is shown in Fig. S1. Where $\delta = 2.00$ ppm is the product methyl proton peak ($-\text{CH}_3$) $\delta = 3.10$ ppm and 3.70 ppm are the product methylene proton peak ($-\text{CH}_2-\text{CH}_2-\text{NH}-$, $-\text{CH}_2-\text{CH}_2-\text{NH}-$), $\delta = 5.25$ ppm and 5.71 ppm are two coupled protons on the vinyl group ($-\text{C}=\text{CH}_2$), $\delta = 7.05$ ppm is the proton on the five-membered indole double bond ($-\text{C}=\text{CH}-$), $\delta = 7.18$, 7.24, 7.42, and 7.66 ppm are four protons on the benzene ring, and $\delta = 5.90$ and 8.22 ppm are the active protons on the imine.

3.2. Characterization of tryptamine and CMC-Na modified polyacrylamide gel

The prepared tryptamine CMC-Na modified acrylamide gel was characterized by FT-IR, SEM, and BET, and

the obtained results are shown below. As shown in Fig. 2a, in the FT-IR spectrum, the gel shows a broad peak near $3,185\text{ cm}^{-1}$, which is a stretching vibration of $-\text{OH}$. Shown at $2,931\text{ cm}^{-1}$ is the stretching vibration of the methylene group. The characteristic absorption peak of fatty ether is displayed at $1,117\text{ cm}^{-1}$. Since, there are no ether bonds in tryptamine and acryloyl chloride, it can be proved that CMC-Na has been doped into the gel component. $1,604$ and $1,448\text{ cm}^{-1}$ are the characteristic absorption peaks of aromatic rings. Among the three main components, only tryptamine has a benzene ring structure, which proves that tryptamine has been doped into the gel system. $1,649\text{ cm}^{-1}$ is the $\text{C}=\text{O}$ stretching vibration of the amide, and $1,412\text{ cm}^{-1}$ is the $\text{C}-\text{N}$ stretching vibration of the amide, both of which are characteristic absorption peaks shared by the acrylamide component and the tryptamine component.

The FT-IR spectrum after adsorption shows that the wavenumber and intensity of some peaks have shifted or changed more than before. Among them, the characteristic peaks of the benzene ring, the imidazole ring, and the carbon-oxygen double bond of the carboxyl group have all changed a lot, which may be the active sites that interact with Fe^{3+} . The imidazole ring and benzene ring react with iron due to the cation- π interaction, while the

carbon-oxygen double bond will undergo a coordination reaction with iron. These functional groups play an important role in the adsorption of iron to the gel. In order to confirm its microstructure and morphology, tryptamine and CMC-Na modified polyacrylamide gel and ordinary acrylamide gel were characterized by SEM, as shown in Fig. 2c and d. In the dry state, the acrylamide hydrogel has an obvious porous structure, and the modified gel also has a porous structure with a denser pore size. At the same time, the long flocculent structure of cellulose can also be observed. According to the results of the BET test, the specific surface area of the modified gel reaches $4.22\text{ m}^2\text{ g}^{-1}$, which is larger than that of the unmodified acrylamide gel ($2.75\text{ m}^2\text{ g}^{-1}$). The results are shown in Fig. S2a and b.

The XPS spectroscopy was used to further explore the chemical composition before and after adsorption, and the results are shown in Fig. S3. In the XPS spectrum, the characteristic signals of carbon ($\text{C } 1\text{s}$, 285.7 eV), nitrogen ($\text{N } 1\text{s}$, 499.2 eV) are very obvious, indicating the successful preparation of the gel. After the adsorption of Fe^{3+} , the binding energy peaks of carbon and nitrogen shifted to the lower energy position, indicating that the indole ring participated in the adsorption process, which was clearly observed in the high-resolution $\text{C } 1\text{s}$ and $\text{N } 1\text{s}$ XPS

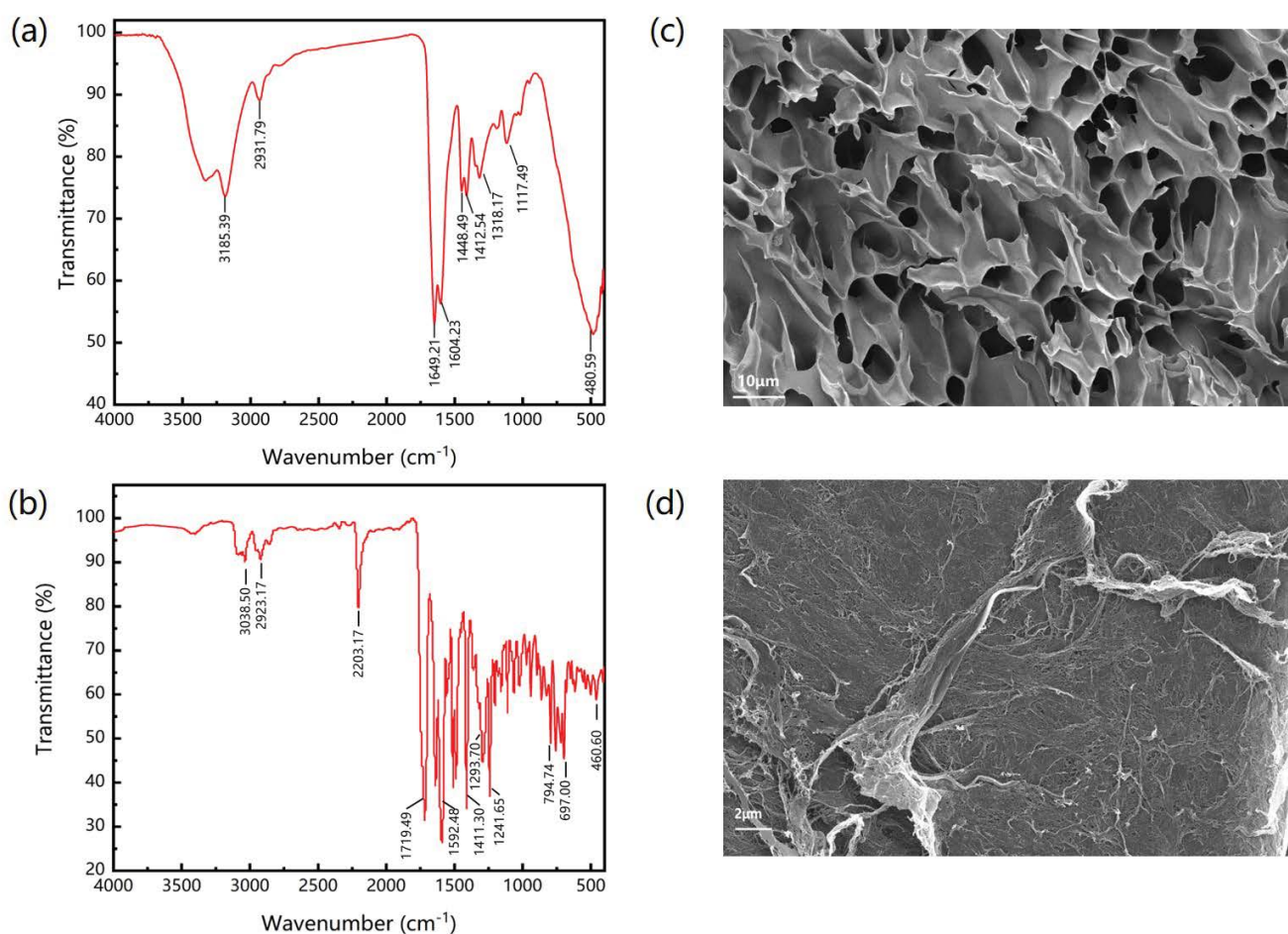


Fig. 2. (a) FT-IR spectrum of the gel without adsorption, (b) FT-IR spectrum of the gel after adsorption of Fe^{3+} , (c) SEM of unmodified gel, and (d) SEM image of modified gel.

spectra. [27] In addition, it can be seen in the XPS spectrum after adsorption that a new peak appears at 712.4 eV and 726.4 eV, indicating that Fe^{3+} is contained after adsorption [28]. Therefore, the XPS results further confirmed that Fe^{3+} was adsorbed by the gel.

3.3. Adsorption experiment

3.3.1. Influence of pH

The pH of the solution is considered to be one of the important parameters affecting the surface charge and chemical properties of the adsorbent and the Fe^{3+} form in the solution, the result is shown in Fig. 3a. Therefore, the pH range in this experiment was from pH = 1 to 3.5. Fe^{3+} with a higher concentration will undergo hydrolysis and agglomeration under weakly acidic conditions to produce insoluble $\text{Fe}(\text{OH})_3$, so the pH higher than 4 was not considered. Under the condition of pH = 1.0–2.0, most of Fe^{3+} was in a free state and the gel surface showed a negative potential. Under this condition, the interaction between the gel and Fe^{3+} is favorable. It can be seen from the results that when the pH was 1.0 and 2.0, both had good adsorption after 24 h, and the best result was when pH = 2.0. When the pH was higher than 3.0, the hydrolysis reaction of Fe^{3+} became violent, and the reaction began to form $\text{Fe}(\text{OH})_3$ deposition. The gel had almost no adsorption effect on $\text{Fe}(\text{OH})_3$ precipitation. Therefore, the adsorption capacity drops sharply to close to zero.

3.3.2. Maximum adsorption capacity test

The adsorption was affected by the initial Fe^{3+} concentration, and the results are shown in Fig. 3b. When the

initial Fe^{3+} concentration changed from 50 to 300 mg L^{-1} , the adsorption capacity gradually increases, showing its excellent adsorption performance. Its maximum adsorption capacity can reach 180 mg g^{-1} , compared with the reports that are mainly based on $-\text{COOH}$, the adsorption capacity of the gel we prepared has increased by nearly 80 mg g^{-1} [29]. The initial concentration of Fe^{3+} provided the necessary driving force to reduce diffusion and interface resistance. The adsorption process of Fe^{3+} was mainly divided into two steps. The first step was to transport the adsorbent molecules from the bulk solution to the outer surface of the adsorbent, and the second step was to transport the adsorbent molecules from the outer surface to the pores of the adsorbent. Therefore, the increase of the initial adsorption concentration could promote the adsorption reaction of tryptamine and CMC-Na modified polyacrylamide gel, improve the interaction between the gel and Fe^{3+} , and make the active adsorption sites on the gel surface react completely.

3.3.3. Contact time

For the adsorption process, we explored the effect of different contact time on the adsorption capacity, the result is shown in Fig. 3c. In the first 2 h, the adsorption rate of the gel increased significantly, and the adsorption capacity reached 100 mg g^{-1} from 0. After 2 h, the adsorption rate decreased, and the adsorption capacity rose slowly to basically unchanged, approaching adsorption saturation. It was shown that within the time period of 2–8 h, the adsorption sites on the gel surface were almost completely reacted, and the remaining adsorption was carried out inside the gel network. Therefore, in

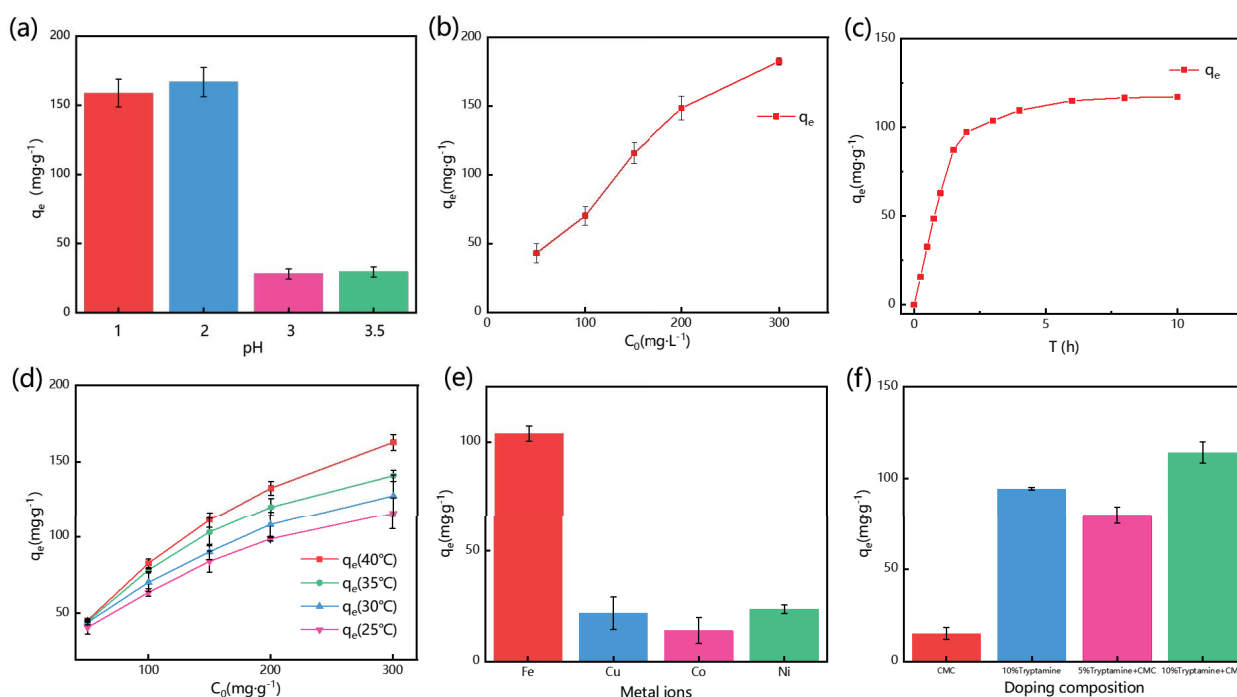


Fig. 3. Effect of (a) pH, (b) initial Fe^{3+} concentration, (c) contact time, (d) temperature, (e) different metal ions, and (f) different composition.

order to show the adsorption effect, we chose 8 h for the subsequent adsorption experiments.

3.3.4. Temperature

We have studied the effect of different initial concentrations of Fe^{3+} on the adsorption at different temperatures in the experiment, and the results are shown in Fig. 3d. In the process of increasing the temperature from 25°C to 40°C , the maximum adsorption capacity of gels with different initial concentrations increased as the temperature increased. This may be because the gel's adsorption of Fe^{3+} is mainly a chemical adsorption process. Increasing the temperature will improve the activity of the adsorption sites on the gel surface, promote the adsorption reaction, and increase the interaction between the indole and carboxyl groups on the Fe^{3+} active sites. In addition, as the temperature increased, the hydrolysis reaction of Fe^{3+} increased, and insoluble $\text{Fe}(\text{OH})_3$ precipitation that is difficult to be absorbed by the gel will be generated. Therefore, the adsorption effect at higher temperatures will decrease.

3.3.5. Selective adsorption

We also studied the adsorption effect of the ions in the solution when there are interfering ions in the solution, and the results are shown in Fig. 3e. A solution containing 200 mg L^{-1} of Co^{2+} , Ni^{2+} , Cu^{2+} , and Fe^{3+} was configured, and the results after 8 h of adsorption are shown in the figure. In the mixed solution, the adsorption capacity of Fe^{3+} reached 100 mg g^{-1} , while the adsorption effect of the other three ions was not obvious, only about 20 mg g^{-1} . It shows the selective adsorption effect of excellent amine CMC-Na modified polyacrylamide gel on Fe^{3+} .

3.3.6. Comparison of modification effects

Four different gels containing different doping components were subjected to Fe^{3+} adsorption for 8 h, and the results are shown in Fig. 3f. The result is shown in the figure. It can be seen from the results that the adsorption capacity of the acrylamide gel containing only CMC-Na is about 15 mg g^{-1} , and the adsorption capacity of the gel containing 10% tryptamine is about 96 mg g^{-1} , 5%. The adsorption capacity of tryptamine and CMC-Na modified

polyacrylamide gel is about 79 mg g^{-1} , and the adsorption capacity of 10% tryptamine and CMC-Na modified polyacrylamide gel is about 115 mg g^{-1} . It can be seen from the results that the combination of the two doping components can not only increase the water absorption of the gel, but also work together to make the gel adsorb Fe^{3+} . At the same time, as the tryptamine component increases, the adsorption capacity will increase to a certain extent.

3.4. Adsorption kinetics

Adsorption kinetics mainly discusses the diffusion performance of the adsorbate on the inner and outer surfaces of the adsorbent, the main influencing factors of the adsorption rate and the speed-limiting steps. The adsorption process is divided into three steps: external diffusion, internal diffusion and surface adsorption. The rate of the slowest stage determines the total rate of adsorption. The relevant parameters of adsorption kinetics are important indicators of the adsorption process and cannot be ignored in the design of the adsorption and separation process, and the results are shown in Fig. 5.

Currently, Lagergren pseudo-first-order kinetic model (PFO), pseudo-second-order kinetic model (PSO), and

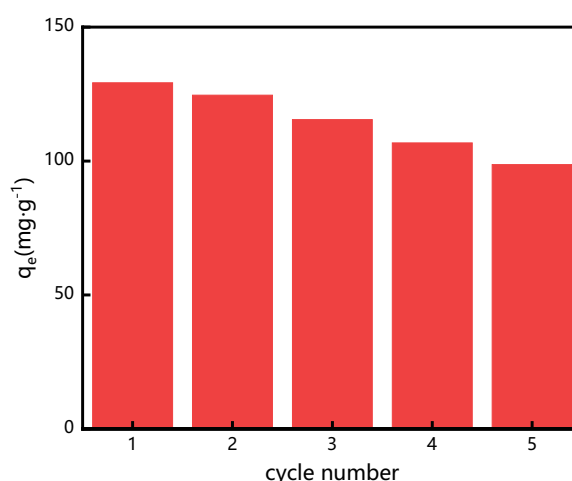


Fig. 5. Cyclability of tryptamine and CMC-Na modified polyacrylamide gel.

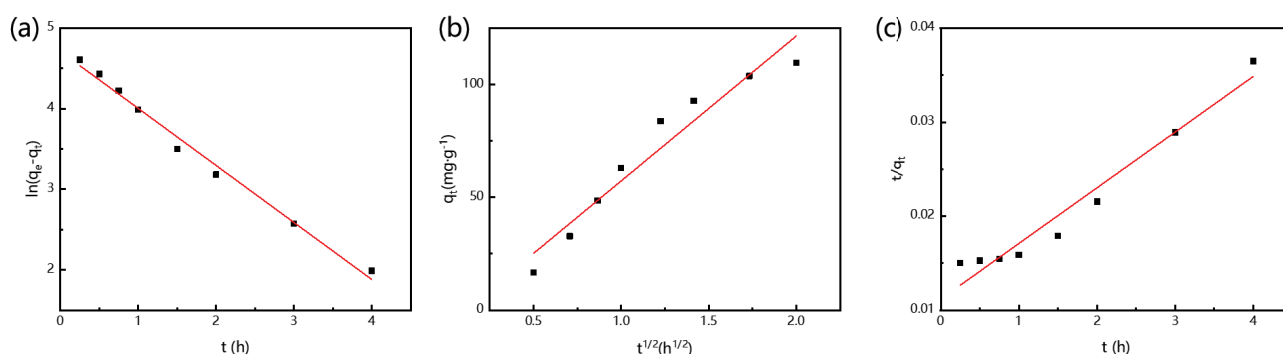


Fig. 4. Kinetics results (a) pseudo-first-order model, (b) intraparticle diffusion model, and (c) pseudo-second-order model.

Webber–Morris intraparticle diffusion model are most commonly used in the adsorption of Fe^{3+} . By comparing the fitting results of different equations, an appropriate model was chosen, preliminary judgment of the adsorption mechanism. In order to explore the adsorption mechanism, the PFO model, PSO model, and intraparticle diffusion model were proposed to fit equilibrium data in this study.

The first-order kinetic model is based on the adsorption capacity of the solid and is suitable for the adsorption kinetic equation of the liquid phase. The linear equation is expressed as follows [30,31]:

$$\frac{dq}{dt} = k_1(q_e - q_t) \quad (2)$$

And rearranged to obtain the following time dependence function:

$$\ln(q_e - q_t) = \ln q_e - k_1 t \quad (3)$$

The pseudo-second-order model is based on the assumption that the rate-limiting step involves chemisorption. The equation is represented as follows:

$$\frac{dq}{dt} = k_2(q_e - q_t)^2 \quad (4)$$

The integrated form of Eq. (4) with the boundary condition can be rearranged and linearized as,

$$\frac{t}{q_t} = \frac{1}{k_2 q_e^2} + \frac{t}{q_e} \quad (5)$$

In order to further clarify the diffusion mechanism, the intraparticle diffusion model was employed to describe the dynamics of the diffusion process and to confirm the steps involved in the adsorption process:

$$q_t = k_i t^{1/2} + c \quad (6)$$

Among them, k_1 (h^{-1}) is the quasi-first-order kinetic constant, k_2 ($\text{g mg}^{-1} \text{h}^{-1}$) is the quasi-second-order kinetic constant, and k_i ($\text{mg g}^{-1} \text{h}^{-1/2}$) is the internal diffusion rate constant. The experimental data fitted to the pseudo-first-order model, intraparticle diffusion model and pseudo-second-order model are shown in Fig. 4. Table 1 lists the parameters (q_e , k_1 , and k_2) and correlation coefficient (R^2) obtained through the regression equation. It can be seen from the table that under the condition of 30°C , the R^2 of the kinetic model fitted by the quasi-first-order model was closer to 1.0, indicating that the adsorption

behavior of Fe^{3+} on tryptamine CMC modified acrylamide gel was more consistent with the standard first-order-model.

3.5. Adsorption isotherm model

Among the adsorption isotherm models, the Langmuir and Freundlich models are the most widely used. The Freundlich model is suitable for the adsorption of uneven surfaces, while the Langmuir model is suitable for the adsorption of uniform surfaces. Langmuir and Freundlich isothermal models were used to investigate Fe^{3+} in tryptamine and CMC-Na modified polyacrylamide gel, in order to analyze the adsorption form energy of tryptamine and CMC-Na modified polyacrylamide gel and explore its adsorption mechanism.

3.5.1. Langmuir adsorption isotherm model

The Langmuir model believes that (I) monolayer adsorption, that is, the range of the unsaturated force field is equivalent to the molecular diameter (2–3 Å); (II) the adsorbent surface is uniform, that is, the adsorption capacity is the same everywhere on the adsorbent surface, and the adsorption heat does not follow the coverage (III) The adsorbed molecules have no force on each other, and the difficulty of adsorption and desorption has nothing to do with whether there are adsorbed molecules around; (IV) Adsorption is dynamic equilibrium, that is, the adsorption and desorption rates are equal after equilibrium is reached. The linearized form of Langmuir adsorption isotherm model is (7) [32].

$$\frac{C_e}{q_e} = \frac{C_e}{q_{\max}} + \frac{1}{q_{\max} b} \quad (7)$$

Among them, q_e and q_{\max} (mg g^{-1}) are the equilibrium and maximum adsorption capacity of the monolayer, respectively, C_e (mg L^{-1}) is the equilibrium concentration of Fe^{3+} , and b (L mg^{-1}) is the Langmuir adsorption constant related to the free energy of adsorption.

3.5.2. Freundlich adsorption isotherm model

The Freundlich isothermal model has no assumptions and can describe single-layer adsorption as well as uneven surface adsorption. Freundlich is also used for adsorption

Table 1
Relevant parameters of the kinetic model of Fe^{3+} adsorption on tryptamine and CMC modified polyacrylamide gel

Pseudo-first-order				Pseudo-second-order		
q_e	k_1	q_e	R^2	k_2	q_e	R^2
116.90	0.7078	111.2	0.9901	0.0012	168.9	0.9596

Table 2
Freundlich and Langmuir model related parameters for the adsorption of Fe^{3+} on tryptamine and CMC modified polyacrylamide gel

T (K)	Freundlich constants			Langmuir constants		
	1/n	K_f	R^2	b	q_{\max}	R^2
298	0.3354	18.55	0.9956	0.0052	155.0	0.9938
303	0.3103	26.08	0.9955	0.0040	142.0	0.9821
308	0.3404	26.40	0.9918	0.0031	133.1	0.9859
313	0.3739	27.19	0.9915	0.0050	182.5	0.9904

Table 3
 ΔG of Fe^{3+} adsorption on tryptamine CMC modified acrylamide gel

T (K)	ΔG (kJ mol ⁻¹)
298	-7.25
303	-8.22
308	-8.382
313	-8.595

in a wide range of concentrations. The Freundlich model cannot calculate the saturated adsorption capacity and the adsorption capacity outside the experimental concentration range. The general form of Freundlich adsorption isotherm is represented in Eq. (8) [33].

$$q_e = KC_e^n \quad (8)$$

Eq. (8) can be linearized in logarithmic form and the Freundlich constants can be determined as follows:

$$\ln q_e = \ln K_F + \frac{\ln C_e}{n} \quad (9)$$

Among them, K_F (mg/g) is related to the affinity of the adsorbent to the adsorbate. The larger the K_F value, the higher the adsorption capacity. n is a constant, which can feedback the difficulty of adsorption and is related to the type, energy distribution and physical and chemical properties of adsorption sites on the adsorbent surface. When $1/n$ is between 0 and 1, the adsorption is easy to proceed. The smaller the $1/n$ value, the stronger the adsorption. When $1/n$ is less than 0.5, it reflects that adsorption is easy to proceed, and when $1/n$ is higher than 2, it is difficult to adsorb. A larger K_F and n mean a sign of good adsorption performance of the adsorbent.

In Table 2, we show the conclusions obtained by using two different models to fit. From the correlation coefficient (R^2), it can be concluded that the two models have good fitting results for the adsorption of Fe^{3+} on tryptamine CMC-modified acrylamide gel, but compared with the Langmuir model, the Freundlich model is more suitable for description, adsorption, and the results are shown in the Fig. S4a and b. In addition, the maximum adsorption capacity (q_{\max}) increases with the increase of temperature, indicating that higher temperature was beneficial to the adsorption of Fe^{3+} on tryptamine and CMC-Na modified polyacrylamide gel, and the adsorption process is endothermic. Moreover, $1/n$ is less than 0.5, which proves that the adsorption of Fe^{3+} by tryptamine and CMC-Na modified polyacrylamide gel was favorable.

3.6. Adsorption thermodynamics

The study of adsorption thermodynamics can clarify the extent and driving force of the adsorption process, and also explain the reasons for the influence of various factors on adsorption. In solid–liquid adsorption, the heat of adsorption is the enthalpy change of the reaction, which is the comprehensive result of the energy change during the adsorption process, and can distinguish between

chemical adsorption and physical adsorption. The calculation process of the three thermodynamic parameters Gibbs free energy (ΔG), enthalpy change (ΔH), and entropy change (ΔS) are as follows [34,35]:

$$\Delta G = -RT \ln K_e^0 \quad (10)$$

$$\ln K_e^0 = \frac{-\Delta H}{RT} + \frac{\Delta S}{R} \quad (11)$$

$$\Delta G = \Delta H - T\Delta S \quad (12)$$

From the previous section, we get that the adsorption isotherm model of tryptamine and CMC-Na modified polyacrylamide gel is more in line with the Freundlich isotherm model, where K_e^0 (mL mg⁻¹) is the thermodynamic equilibrium constant of Freundlich isotherm model, R is the universal gas constant (8.314 J mol⁻¹ K⁻¹) and T is the temperature (K). According to Eqs. (10) and (11), we can calculate the value of ΔG at different temperatures, and the results are shown in Table 3.

Plot the logarithm of K_e^0 and the reciprocal of temperature, a straight line can be obtained, and the enthalpy change and entropy change of the reaction can be obtained according to the slope and intercept of the linear equation.

The negative value of ΔG decreases with increasing temperature, indicating that adsorption was a spontaneous process, and the higher temperature was more conducive to adsorption. The fitting result is shown in Fig. S5. The enthalpy (ΔH) was calculated to be 17.53 KJ mol⁻¹, which was positive, indicating that the adsorption was an endothermic process. The exothermic adsorption process is usually physical adsorption or chemical adsorption, while the endothermic process is chemical adsorption. Therefore, the positive value of ΔH further confirms that the adsorption of Fe^{3+} is chemical adsorption, rather than physical adsorption. The ΔS is calculated to be 0.084 kJ K⁻¹ mol⁻¹, which was a positive value indicating that the prepared gel had a good affinity for Fe^{3+} .

3.7. Recyclability of tryptamine and CMC-Na modified polyacrylamide hydrogel

The recyclable adsorbent has a very important significance for enhancing reduce material costs and improve its economic efficiency. In order to evaluate the recyclability of the tryptamine and CMC-Na modified polyacrylamide hydrogel, we explored the adsorption and regeneration of the gel. There is a good coordination interaction between EDTA and Fe^{3+} , so we choose 0.3 mol/L EDTA as the desorption agent. The results are shown in Fig. 5. Under the conditions of constant adsorption temperature, Fe^{3+} concentration and time, the adsorption capacity gradually decreases slightly as the cycle number increases. When hydrogel is recycled 5 times, the adsorption capacity of the regenerated tryptamine and CMC-Na modified polyacrylamide hydrogel for Fe^{3+} is 23.7% lower than that of the initial, indicating that the adsorption effect of hydrogel decreases slightly with regeneration and repeated use, but it does not cause significant loss.

4. Conclusion

In this project, polyacrylamide hydrogel was used as the base material, tryptamine is used for functional modification, and CMC-Na was used to form a gel network, and a gel with excellent Fe³⁺ adsorption capacity was synthesized. The indole structure of tryptamine and the carboxyl structure of CMC-Na together promote the adsorption effect of iron ions. The optimal conditions for the gel's adsorption of Fe³⁺ were explored by controlling variables, and the adsorption mechanism was analyzed and fitted, which confirmed that the synthesized gel had good adsorption capacity. Therefore, we can be sure that tryptamine CMC-Na modified polyacrylamide gel is an excellent iron wastewater purification material, and has broad application prospects in the Fe³⁺ treatment of domestic sewage and industrial wastewater.

Acknowledgements

This work was supported by the Laser Fusion Research Center Funds for Young Talents (no. RCFCZ1-2017-16), Applied Basic Research Program of Sichuan Province (no. 2019YJ003), and State Key Laboratory of Environment-friendly Energy Materials (no. 19kfhg01).

References

- M. Sajid, M.K. Nazal, N. Baig, A.M. Osman, Removal of heavy metals and organic pollutants from water using dendritic polymers based adsorbents: a critical review, *Sep. Purif. Technol.*, 191 (2018) 400–423.
- H. Karadede, E. Ünlü, Concentrations of some heavy metals in water, sediment and fish species from the Atatürk Dam Lake (Euphrates), Turkey, *Chemosphere*, 41 (2000) 1371–1376.
- L. Stegpnjak, U. Kegpa, E. Stan'czyk-Mazanek, The research on the possibility of ultrasound field application in iron removal of water, *Desalination*, 223 (2008) 180–186.
- N. Khatri, S. Tyagi, D. Rawtani, Recent strategies for the removal of iron from water: a review, *Water Process Eng.*, 19 (2017) 291–304.
- P. Maneechakr, S. Karnjanakom, The essential role of Fe(III) ion removal over efficient/low-cost activated carbon: surface chemistry and adsorption behavior, *Res. Chem. Intermed.*, 45 (2019) 4583–4605.
- D. Ghosh, H. Solanki, M.K. Purkait, Removal of Fe(II) from tap water by electrocoagulation technique, *J. Hazard. Mater.*, 155 (2008) 135–143.
- D. Ellis, C. Bouchard, G. Lantagne, Removal of iron and manganese from groundwater by oxidation and microfiltration, *Desalination*, 130 (2000) 255–264.
- K. Vaaramaa, J. Lehto, Removal of metals and anions from drinking water by ion exchange, *Desalination*, 155 (2003) 157–170.
- R. Munter, H. Ojaste, J. Sutt, Complexed iron removal from ground water, *J. Environ. Eng.*, 131 (2005) 1014–1020.
- S. Vasudeva, Effects of alternating current (AC) and direct current (DC) in electrocoagulation process for the removal of iron from water, *Can. J. Chem. Eng.*, 90 (2012) 1160–1169.
- S. Vasudevan, J. Jayaraj, J. Lakshmi G. Sozhan, Removal of iron from drinking water by electrocoagulation: adsorption and kinetics studies, *Korean J. Chem. Eng.*, 206 (2007) 251–258.
- M. Ghashghaee, Z. Azizi, M. Ghambarian, Adsorption of iron(II, III) cations on pristine heptazine and triazine polymeric carbon nitride quantum dots of buckled and planar structures: theoretical insights, *Adsorption*, 26 (2020) 429–442.
- D. Savova, N. Petrow, M.F. Yardim, The influence of the texture and surface properties of carbon adsorbents obtained from biomass products on the adsorption of manganese ions from aqueous solution, *Carbon*, 41 (2003) 1897–1903.
- E. Okoniewska, J. Lach, M. Kacprzak, E. Neczaj, The removal of manganese, iron and ammonium nitrogen on impregnated activated carbon, *Desalination*, 206 (2007) 251–258.
- T. Henkel, R.M. Brunne, H. Muller, F. Reichel, Statistical investigation into the structural complementarity of natural products and synthetic compounds, *Angew. Chem. Int. Ed.*, 38 (1999) 643–647.
- J. Kim, M. Movassaghi, Biogenetically inspired syntheses of alkaloid natural products, *Chem. Soc. Rev.*, 38 (2009) 3035–3050.
- M. Bandini, A. Eichholzer, Catalytic functionalization of indoles in a new dimension, *Angew. Chem. Int. Ed.*, 48 (2009) 9608–9644.
- N.K. Kaushik, N. Kaushik, P. Attri, N. Kumar, C.H. Kim, A.K. Verma, E.H. Choi, Biomedical importance of indoles, *Molecules*, 18 (2013) 6620–6662.
- G. Chang, L. Yang, J. Yang, M.P. Stoykovich, X. Deng, J. Cui, D. Wang, High-performance pH-switchable supramolecular thermosets via cation- π interactions, *Adv. Mater.*, 30 (2018) 1704234, doi: 10.1002/adma.201704234.
- W. Wei, G. Chang, Y. Xu, L. Yang, An indole-based conjugated microporous polymer: a new and stable lithium storage anode with high capacity and long life induced by cation- π interactions and a N-rich aromatic structure, *J. Mater. Chem. A*, 6 (2018) 18794–18798.
- G. Chang, Z. Shang, T. Yu, L. Yang, Rational design of a novel indole-based microporous organic polymer: enhanced carbon dioxide uptake via local dipole- π interactions, *J. Mater. Chem. A*, 4 (2016) 2517–2523.
- G. Chang, L. Yang, J. Yang, Y. Huang, K. Cao, J. Ma, D. Wang, A nitrogen-rich, azaindole-based microporous organic network: synergistic effect of local dipole- π and dipole-quadrupole interactions on carbon dioxide uptake, *Polym. Chem.*, 7 (2016) 5768–5772.
- L. Zhang, L. Yang, Y. Xu, G. Chang, Renewable 4-HIF/NaOH aerogel for efficient methylene blue removal via cation- π interaction induced electrostatic interaction, *RSC Adv.*, 51 (2019) 29772–29778.
- Y. Wang, L. Zhang, L. Yang, G. Chang, An indole-based smart aerogel for simultaneous visual detection and removal of trinitrotoluene in water via synergistic effect of dipole- π and donor-acceptor interactions, *Chem. Eng. J.*, 384 (2020) 123358–123366.
- E.S. Abdel-Halim, S.S. Al-Deyab., Preparation of poly(acrylic acid)/starch hydrogel and its application for cadmium ion removal from aqueous solutions, *React. Funct. Polym.*, 75 (2014) 1–8.
- C.A. Cima-Mukul, M.T. Olguin, M. Abatal, J. Vargas, J.A. Barron-Zambrano, A. Avila-Ortega, A.A. Santiago, Assessment of *Leucaena leucocephala* as bio-based adsorbent for the removal of Pb²⁺, Cd²⁺ and Ni²⁺ from water, *Desal. Water Treat.*, 173 (2020) 331–342.
- M.A. Oliver-Tolentino, J. Vazquez-Samperio, A. Manzo-Robledo, R. de G. Gonzalez-Huerta, J.L. Flores-Moreno, D. Ramirez-Rosales, A. Guzman-Vargas, An approach to understanding the electrocatalytic activity enhancement by superexchange interaction toward OER in alkaline media of Ni-Fe LDH, *J. Phys. Chem. C*, 118 (2014) 22432–22438.
- F. Geneste, M. Cadoret, C. Moinet, G. Jezequel, Cyclic voltammetry and XPS analyses of graphite felt derivatized by non-Kolbe reactions in aqueous media, *New J. Chem.*, 26 (2002) 1261–1266.
- H. Zhai, D. Li, M. Li, J. Zou, Acylation modification of konjac glucomannan and its adsorption of Fe(III) ion, *Carbohydr. Res.*, 497 (2020) 108133–108140.
- R. Kamaraj, A. Pandiarajan, M. Rajiv Gandhi, Eco-friendly and easily prepared graphene nanosheets for safe drinking water: removal of chlorophenoxyacetic acid herbicides, *2* (2017) 342–355.
- R. Kamaraj, S. Vasudevan, Facile one-pot synthesis of nano-zinc hydroxide by electro-dissolution of zinc as a sacrificial

anode and the application for adsorption of Th^{4+} , U^{4+} , and Ce^{4+} from aqueous solution, *Res. Chem. Intermed.*, 42 (2016) 4077–4095.

- [32] S. Vasudevan, J. Lakshmi, Process conditions and kinetics for the removal of copper from water by electrocoagulation, *Environ. Eng. Sci.*, 29 (2012) 563–572.
- [33] S. Vasudevan, J. Lakshmi, G. Sozhan, Optimization of the process parameters for the removal of phosphate from drinking water by electrocoagulation, *Desal. Water Treat.*, 12 (2009) 407–414.

[34] Z. Lei, W. Gao, J. Zeng, B. Wang, J. Xu, The mechanism of $\text{Cu}(\text{II})$ adsorption onto 2,3-dialdehyde nano-fibrillated celluloses, 230 (2020) 115631–115638.

[35] S. Vasudevan, J. Lakshmi, Studies relating to an electrochemically assisted coagulation for the removal of chromium from water using zinc anode, *Water. Sci. Tech.-Water Supply*, 11 (2011) 142–150.

Supplementary information

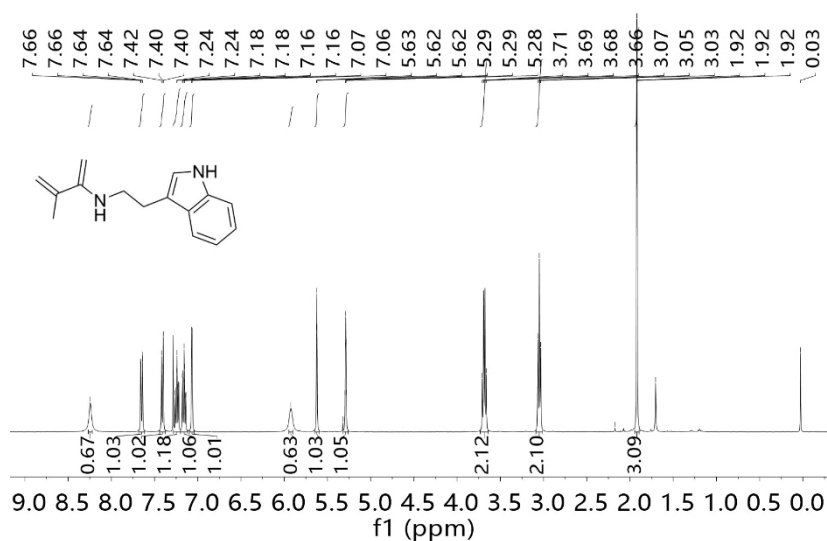


Fig. S1. $^1\text{H-NMR}$ spectrum of N-(2-(1H-indol-3-yl)ethyl)methacrylamide.

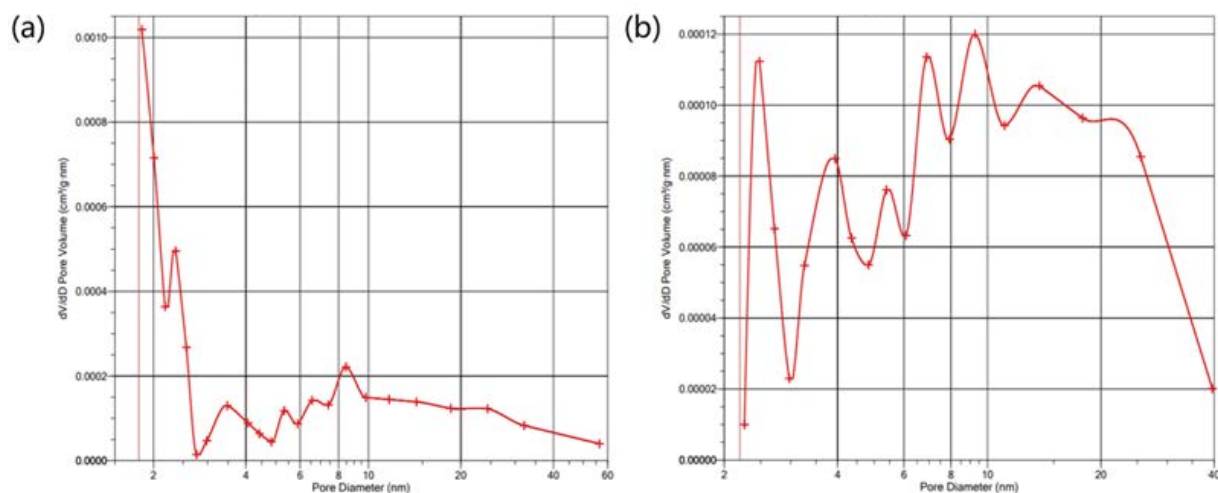


Fig. S2. BET specific surface area test curve of (a) polyacrylamide gel and (b) tryptamine and CMC-Na modified polyacrylamide gel.

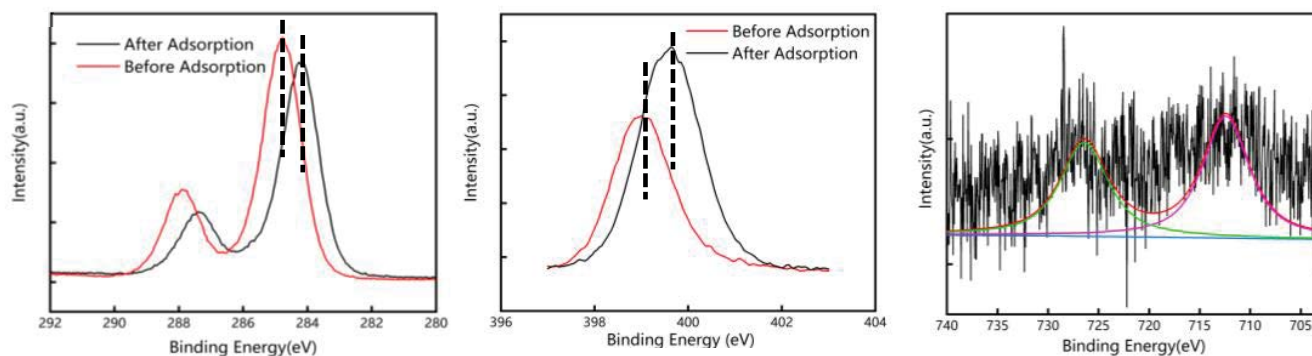


Fig. S3. Before and after gel adsorption of Fe³⁺ (a) XPS spectrum of C1s, (b) XPS spectrum of N1s, and (c) XPS spectrum of Fe³⁺ 2p after adsorption.

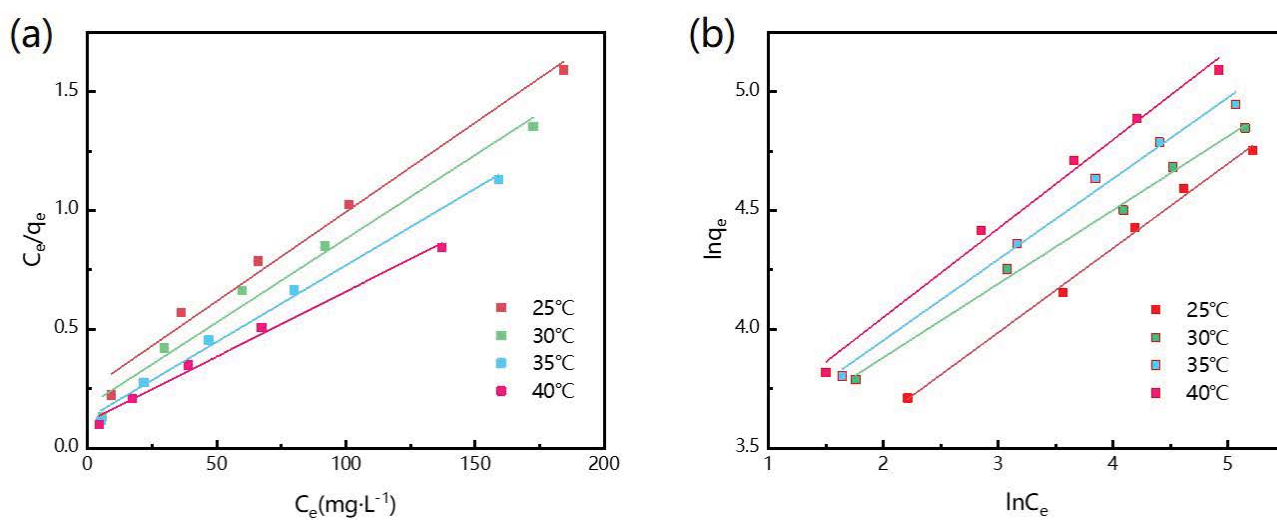


Fig. S4. Fitting results of the isothermal model for Fe³⁺ adsorption by tryptamine and CMC modified polyacrylamide gel, (a) Langmuir model and (b) Freundlich model.

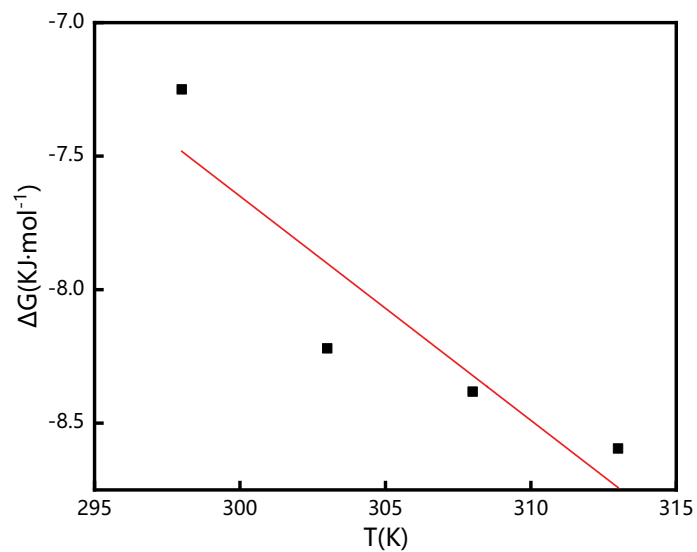


Fig. S5. Fitting results of adsorption thermodynamics.